POLITECNICO DI TORINO
Repository ISTITUZIONALE

Experimental analysis of the start-up of a natural circulation loop in single and two-phase flow

(Article begins on next page)

10 April 2024

EXPERIMENTAL ANALYSIS OF THE START-UP OF A NATURAL CIRCULATION LOOP IN SINGLE AND TWO-PHASE FLOW

C. Bertani, A. Bersano, M. De Salve, G. Sobrero

Dipartimento Energia, Politecnico di Torino, Corso Duca degli Abruzzi 24, 10129 Torino, Italy

Corresponding author:
Cristina Bertani (<u>cristina.bertani@polito.it</u>)

ABSTRACT

With reference to passive heat removal systems for advanced nuclear reactors, an experimental campaign has been carried out to study the start-up of a natural circulation loop in single and two-phase flow. The effect of the heat source power and initial mass inventory have been investigated. The facility consists of a loop 4.828 m high and 10.275 m long, that includes an electrically heated bayonet heat exchanger and a pool heat sink, and can operate at a maximum pressure of 20 bar. Both single- and two-phase flow (air and water) have been tested and typical oscillations have been observed. Characteristic transient phases have been defined by analyzing the time histories of pressures, temperatures and flow rate in the loop and in the water pool. During the transients, the bayonet heat-up phase is followed by a phase of natural circulation activation, then a natural circulation development phase and, in some tests, a nearly steady-state phase. The duration of the phases has been studied with different mass inventories and heat source power. It has been observed that the natural circulation is established more quickly at higher power; the final pressure increases with the power and decreases with the mass inventory. The natural circulation flow rate at the end of the transients depends on the heat source power, with a small influence of the mass inventory value. At high water filling of the loop, single-phase natural circulation is developed, a fast pressure transient occurs and the pressure in the loop has a diverging behavior. At lower water fillings, two-phase two-component flow (air, water and steam) occurs and the system pressure tends to reach a near-steady-state value.

KEYWORDS
Heat removal; nuclear reactors safety; passive systems; natural circulation; start-up phase.

1. INTRODUCTION

Natural circulation systems have already found application in many industrial fields, such as the chemical and nuclear ones, and the physical mechanism has been investigated for many years. Recently, natural circulation became a key element for the safety of nuclear plants and it is being adopted to passively remove heat in advanced nuclear reactors (e.g. Westinghouse AP1000 [1], General Electric ESBWR [2][3]), Small Modular Reactors (SMR) [4] and Generation IV reactors [5]. Some natural circulation systems are designed to be used in normal operating conditions for the removal of the heat generated by the chain reaction, others for the removal of the decay heat in normal conditions or accidental conditions, including Design Basis Accidents and also Beyond-Design Basis Accidents. These natural circulation systems can be of direct or indirect type, if the natural circulation occurs in the primary coolant (such as in the ESBWR, NuScale SMR,

CAREM SMR, SMART SMR, Gen-IV Lead-cooled Fast Reactor, etc.) or in a secondary loop (such as the Passive Residual Het Removal Systems of AP1000, EPR, IPWR, HPR1000, etc.)

The driving force in natural circulation systems, which is due to the presence of fluids with different densities in a hot leg and a cold leg, is much smaller than in forced circulation systems; therefore, the flow rate along a natural circulation loop is normally much lower than in a forced circulation one. The driving force increases with the loop height, depends on the power of the heat source and, during transients, it is also influenced by the inertia of the fluid in the pipes and heat capacity of the solid structures.

Natural circulation is being studied since long time both theoretically and experimentally [6]. Extensive studies regarded the single-phase natural circulation. Vijayan et al. analysed steady-state single-phase natural circulation both experimentally and theoretically, developing scaling laws [7] and highlighting the effect on the circulating flow rate of the loop geometry and power provided to the heated section. They also analysed instabilities in natural circulation flow [8-12] and developed stability maps using modified Grashof and Stanton numbers. Pini et al. [14] extended the analysis of single-phase natural circulation flow to internally heated fluids (exothermic reagents or nuclear liquid fluids): the authors developed an analytical model and compared its results with numerical models developed by Dymola, Openfoam and RELAP5.

It is also well-known that boiling systems can suffer from instabilities [15-16].

Several researchers have already emphasized that flow instabilities could arise in natural circulation when the transition from single-phase to two-phase flow regime occurs, especially in low pressure natural circulation systems. Some recent experimental and numerical analyses are reported in [17-21].

Since natural circulation systems are also foreseen for the heat removal from the containment, the operating pressure can range from the nominal values of the primary system, in the reactor operating conditions, down to atmospheric pressure. Flow instabilities can induce oscillations in the thermal-hydraulic parameters that could cause dangerous mechanical vibrations, pipes breakdown, thermal crisis in the heated channels and core damage. Moreover, the occurrence of instabilities may hinder or delay the natural circulation development.

Several studies have been carried out on the start-up of boiling water reactors [22-26]. The study of the start-up phase of natural circulation is fundamental also for those indirect systems that are in stand-by conditions during normal operation, and are required to operate in accidental conditions.

Best estimate codes have been used to simulate the performance of passive residual heat removal systems in accidental conditions [27-33]. Some experimental data are available on two-phase natural circulation for the passive removal of the decay heat, but experimental studies are still needed at relatively low pressure. Moreover, the capabilities of computational models and system codes should be validated at the operating conditions of the new systems, which often include pools at nearly atmospheric pressure.

The present paper concerns the natural circulation in a small closed loop, initially at ambient conditions, when a step of power is applied on the outer surface of the heat source.

The experimental campaign has been carried out using the facility PROPHET2, built and operated at Dipartimento Energia of Politecnico di Torino, which is a modification of the PROPHET facility [34-36], a reduced-height, reduced-pressure test facility inspired to the second Decay Heat Removal system (DHR) of ALFRED reactor [37]. In liquid metal cooled reactors, being the heat sink of the DHR at a temperature lower than the liquid metal solidification temperature, the safe operation of the DHR also involves the need to avoid the coolant freezing in the long term, which would generate obstructions in the natural circulation flow of the primary coolant.

ALFRED reactor adopts an innovative DHR system able to passively control the power extracted from the primary coolant; the system contains water that heats-up and boils in bayonet heat exchangers submerged into the liquid metal pool and condenses in an isolation condenser submerged into a water pool. The isolation condenser is connected to a tank containing nitrogen, which would be passively released into the DHR loop and induces a reduction of the condensation heat transfer coefficient in the isolation condenser and therefore a decrease of rate of temperature reduction in the DHR loop. The presence of non-condensable gases within the water passively controls the heat removal from the primary coolant and avoids its freezing in the long term [37, 38].

The main aims of this experimental study are the classification of transients of start-up of natural circulation, together with the individuation of phenomenological windows and their characteristic times as function of initial and boundary conditions.

The experimental campaign allows to study the phenomena occurring during different phases of the activation and development of natural circulation in a system initially in stand-by conditions at ambient temperature and pressure, and analyze the effects of the presence of non-condensable gases on the start-up of the system and on thermal-hydraulic conditions in the longer term.

In particular, this work analyzes the effects of power and initial mass of water in the closed loop on the natural circulation development in terms of pressures, temperatures and flow rate time behaviours for specific loop characteristics (components heights and volumes, walls heat capacity, heat transfer surface with the environment and heat sink).

The geometry of the system, together with the initial pressure and temperature and boundary conditions can strongly influence the natural circulation start-up. The transient flow rate depends on the difference between the densities of water in the cold and hot leg, the height difference between the heat source and the heat sink, length to diameter ratios of the components and geometrical singularities.

To translate results to industrial applications with different geometries and operating conditions, scaling laws should be applied [39,40].

The experimental results of the present campaign may also be useful to validate system codes typically used for the safety analysis of nuclear reactors equipped with passive heat removal systems that include innovative components and that often operate at thermal-hydraulic conditions different from the ones for which the codes were originally been developed.

The experimental facility includes a bayonet heat exchanger that operates as heat source, while the heat sink is represented by a vertical straight pipe submerged in a small size water pool initially at ambient temperature (with an initial water level of approximately 0.45 m), and the distributed heat losses from the loop components to the ambient. The whole transient is studied, from the start-up phase up to a possible nearly steady-state condition.

The experimental facility, the instrumentation, the test procedure and experimental matrix are reported in Section 2.

Section 3 presents the experimental results. The experimental transient is divided in typical time intervals. The phenomena occurring in each time interval are described. The effects of the loop filling and the power provided to the heat source on the main parameters during the different time intervals and phenomenological windows are also discussed.

Finally, conclusions and hints for future work are reported in Section 4.

2. TEST FACILITY AND EXPERIMENTAL CAMPAIGN

2.1. Test facility

The experimental facility is schematically represented in Fig. 1.. It mainly consists of an electrically heated bayonet heat exchanger (BHX) located at the lowermost position, a pipe (heat sink, HS) immersed in a water pool (HSWP) at a higher elevation, the hot leg pipe (HL) connecting the bayonet heat exchanger outlet to the heat sink inlet, the cold leg pipe (CL) connecting the heat sink outlet to the bayonet inlet, a water reservoir (WR) connected to the HSWP and valves. The BHX together with HL, CL, and HS constitute a closed loop, whose total height is 4.828 m. The distance between the axis of the two vertical pipes is 0.364 m.

The loop is connected to a vertical safety valve (SV; V05 in Fig. 1) and to a horizontal pneumatic valve (PV; V04 in Fig. 1)). The connection pipes to the SV and PV, together with these two valves is named Upper Volume (UV) and behaves similarly to a close expansion volume.

Figure 1 also reports the elevation of the components, expressed in mm, with respect to the inner surface of the bottom of the BHX.
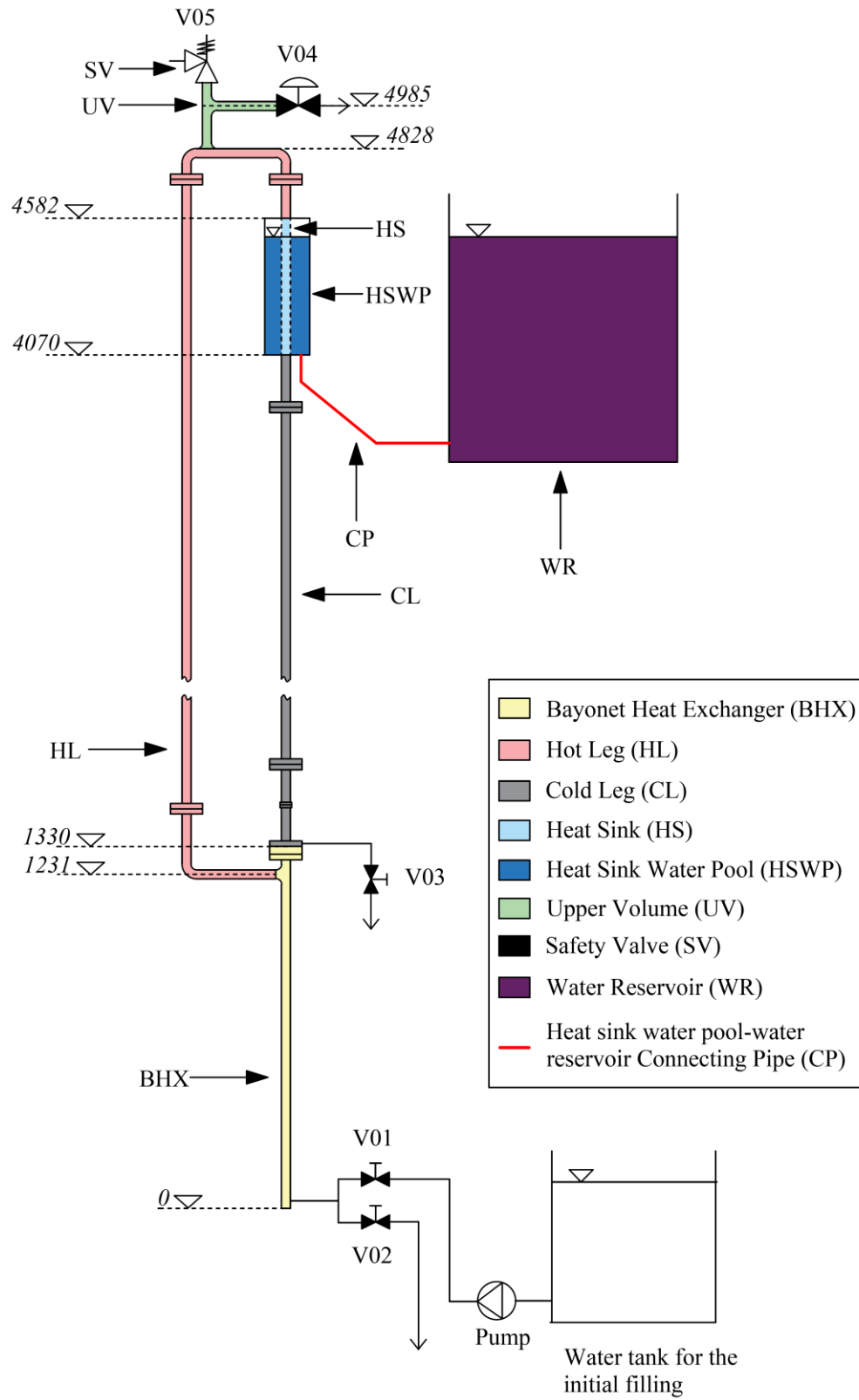
Figure 1. Schematic view of the experimental facility with components elevations (in mm).

The opening pressure of the SV has been set to 20 bar to avoid inadvertent overpressures in the system; the SV never opened during the present experimental campaign, since the tests were stopped before the setpoint pressure was reached.

The total volume of the facility is approximately 3.123 dm^3, while the volume of the loop and of the UV are respectively 2.949 dm^3 and 0.174 dm^3. The volume of the closed loop (that includes BHX, HL, HS, CL) is 94.4% of the total facility volume.

All the loop components are made of stainless steel AISI 304 (density=7930 kg/m^3; specific heat capacity=0.5 kJ/kg/K; thermal conductivity=16 W/m/K). Table I summarizes height and volume of the different components.

The bayonet heat exchanger consists of two coaxial pipes: the fluid enters the bayonet from the top, it flows downwards along the inner pipe (downcomer), then the fluid inverts its motion in the inversion chamber and flows upwards in the annulus, where it receives heat from the outer bayonet wall. The downcomer has inner and outer diameters of 8 mm and 10 mm respectively and a length of 1.32 m. The outer pipe (d_{in}=20.7 mm, d_{out}=33.4 mm, 1" SCH 160) is electrically heated by 10 straight electric resistances (nominal power 800 W each) longitudinally mounted on the bayonet outer surface.

The inversion chamber at the bayonet bottom is 15 mm high. The bayonet downcomer and annulus form a U-tube configuration.

The hot leg, the heat sink and the cold leg consist of pipes with an inner diameter of 20.7 mm and an outer diameter of 33.4 mm (1" SCH 160). The hot leg includes a horizontal pipe at the bayonet outlet, a vertical pipe (riser), a horizontal pipe at the top of the loop and another vertical pipe upstream the heat sink inlet. The cold leg consists of the pipe connecting the outlet of the heat sink to the bayonet downcomer.

The heat transfer areas of the hot and cold legs are different, since different pipe length are involved. Moreover, the hot leg is insulated with a 3 cm thick rockwool layer from the bayonet outlet until the horizontal pipe downstream the riser; on the contrary, the cold leg pipe is bare.

The flanges used to connect pipes and components are 120 mm in diameter and 20 mm in thickness.

The HSWP is a cylinder with a inner diameter of 0.164 m and a height of 0.512 m, which surrounds the heat sink pipe. The HSWP is open to the atmosphere, but its top is provided with a deflector to prevent both the contact of steam produced in the pool with the outer surface of the pipes just upstream the heat sink tube and the spread of liquid outside the pool when the pool water heavily boils.

The bottom of the HSWP is connected by a pipe (CP) to the water reservoir, which is a stainless steel AISI 304 tank with height 1 m, width 0.85 m and depth 1.2 m (outer dimensions). The HSWP pool together with the water reservoir forms a U-tube configuration. The water of the HSWP that evaporates during the tests is compensated by the water reservoir.

Table I. Geometrical characteristics of components

Component	Height [m]	Length [m]	Volume [m^3*10^{-3}]	Component Volume/Facility volume
Bayonet	1.328	1.328	0.394	0.126
Hot leg	3.351	4.499	1.482	0.475
Heat sink ("condenser")	0.512	0.512	0.169	0.054
Cold leg	2.74	2.74	0.904	0.289
Upper volume with safety valve	0.246	0.502	0.174	0.056
Water pool (heat sink)	0.512	0.512	10.27	-

2.2. Instrumentation and data acquisition

The measured parameters are absolute pressures, differential pressures, fluid and wall temperatures, water mass and the power provided to the electric heaters by four adjustable autotransformers. Three autotransformers provide a fixed voltage, each of them to a couple of electric heaters; the forth autotransformer feeds a group of four electric resistances. The electric resistance of each electric heater is approximately 78Ω, with an uncertainty of 10%.

The most important absolute pressure values are measured at the bottom (p_1) and near the top (p_2) of the loop (Fig. 2) and at the bottom of the water reservoir (p_3), which is used to evaluate the liquid level height in the water reservoir.

The differential pressure through an orifice (Δp_4) is used to derive the flow rate in the loop. The flow meter spool is placed upstream the bayonet inlet and contains an orifice designed, built and calibrated at Politecnico di Torino. Differential pressures are also measured along the riser (Δp_2), the cold leg (Δp_3), across the bayonet heat exchanger (Δp_1), across the heat sink tube (Δp_6). All the pressure transducers are of industrial type and have an accuracy of 1% of Full Scale (FS) in the range 30%-100% of Full Scale (FS). The instrument FS values are reported in Table II.

The output of the absolute pressure transducers is a tension in the range 0-10 V, while the output of differential pressure transducers is a current in the range 4-20 mA.

The signals are acquired by the Data Acquisition System (DAS) and converted in pressure using the calibration curve of each instrument.

Voltage and current at the electric heaters are measured with an accuracy of 1V and 0.1 A respectively, with corresponds to a relative uncertainty on the power of approximately 1.2% at 2500 W, and 0.84% at 5000W.

Fluid temperatures along the loop (T1-9) and in the water pool (TP1-3) and wall temperatures of the outer surface of some components (TWA-H) are measured by K-type thermocouples (static uncertainty ±1.1 K), while electric heater temperatures at their upper end are measured by J-type thermocouples (static uncertainty ±2 K).

The K-type thermocouples were tested before the installation in the facility. They were submerged in melting ice and signals were acquired by the DAS: the maximum discrepancy between the values of temperature was ±1 K.

Considering as origin the position of thermocouple T8 and following the clockwise direction, the curvilinear coordinates of the fluid temperatures T8, T1, T2, T3, T4, T5, T6, T9 and T7 are respectively 0.0 m, 1.374 m, 2.643 m, 3.223 m, 6.317 m, 7.017 m, 7.639 m, 7.864 m, 9.949 m; the total curvilinear length of the loop is 10.275 m.

Water masses are measured by a scale with accuracy 0.001 kg and FS 10 kg.

Table II Pressure transducers characteristics and standard deviation in cold conditions (0-60 s)

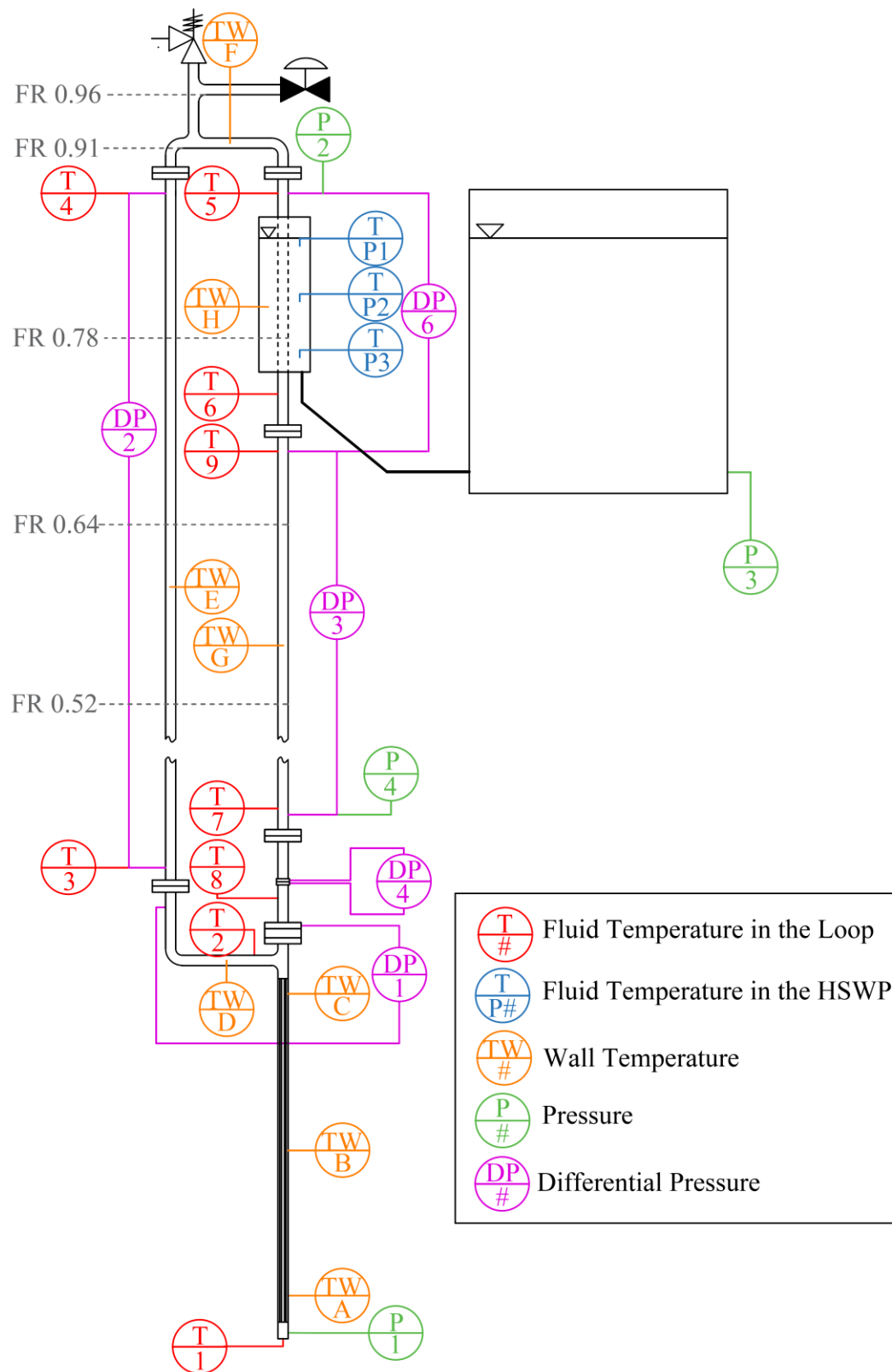|	Full Scale	Accuracy	Standard Deviation
p_1 (bar)	30	0.3	0.357
p_2 (bar)	30	0.3	0.326
p_3 (mbar)	750	0.765	0.608
Δp_1 (mbar)	±630	6.300	4.620
Δp_2 (mbar)	±310	3.100	1.640
Δp_3 (mbar)	1250	12.500	2.860
Δp_4 (mbar)	50	0.500	0.217
Δp_6 (mbar)	400	4.000	1.565

Figure 2. Schematic view of the experimental facility with the measurement points.

The DAS consists of two NI 9213 modules for the thermocouples, a NI 9203 module for the current measurements and a NI 9205 module for the voltage measurements connected to a NI cDAQ 9174. The data acquisition sampling rate is 1 Hz for temperatures and 4 Hz for pressures.

At the beginning of each test, the signals from all the transducers are recorded for 60 s. The acquired data allow the evaluation of amplitude of oscillations due to electronics and A/D conversion; the standard deviation with respect to the mean values during the first 60 s are reported in Table II.

The measured parameters allow to evaluate pressure changes in the various components of the loop, and the water thermal-hydraulic conditions.

The fluid temperature profile along the axial curvilinear coordinate of the loop, evaluated at different fixed times, provides interesting information on the time evolution of the experimental transients and on the power exchanged by the fluid in the different section of the loop.

2.3. Orifice Calibration tests

The orifice used for the measurement of the flow rate has been calibrated in single-phase flow at ambient temperature by forcing through it a flow rate of 5-45 g/s of water. Pressure and temperature of the water were also measured at the spool piece inlet. The water flow rate, measured by the weighing method, is represented versus the differential pressure Δp_4 in Fig.3.

In order to evaluate the flow rate at the pressure and temperature conditions occurring during the tests, the following correlation was used [41]:

$$F = \alpha \varepsilon \frac{\pi d^2}{4} \sqrt{2\rho \Delta p_4}$$

where F is the mass flow rate (kg/s), α the flow rate coefficient, ε the compressibility coefficient (equal to 1 for liquid), d the orifice throat diameter (m), ρ the fluid density and Δp_4 the pressure drop across the orifice.

The flow rate coefficient if given by:

$$\alpha = \frac{C}{\sqrt{1 - \beta^4}}$$

Where: $= \frac{d}{D}$, with D= pipe inner diameter

$$C = 0.5959 + 0.0312\beta^{2.1} - 0.184\beta^8 + 0.0029\beta^{2.5} \left(\frac{10^6}{Re_D}\right)^{0.75}$$

Figure 3 also shows the values predicted by this formula using the nominal throat diameter (5 mm).

The discrepancy with respect to the experimental values could be due to the drilling process of the orifice hole, resulting in a slightly bigger throat diameter. A parametric study has been carried out to find the value of the throat diameter that allows to best predict the actual flow rate. The most suitable value resulted to be 5.5 mm; this value was therefore used in order to evaluate the flow rate during the experimental campaign. This model provides reliable values of the flow rate only in tests with single-phase flow.

Considering an uncertainty of 0.5 mbar on the pressure drop and of 1°C on the temperature, the uncertainty on the flow rate in the calibration tests is $6 \cdot 10^{-5}$ kg/s.
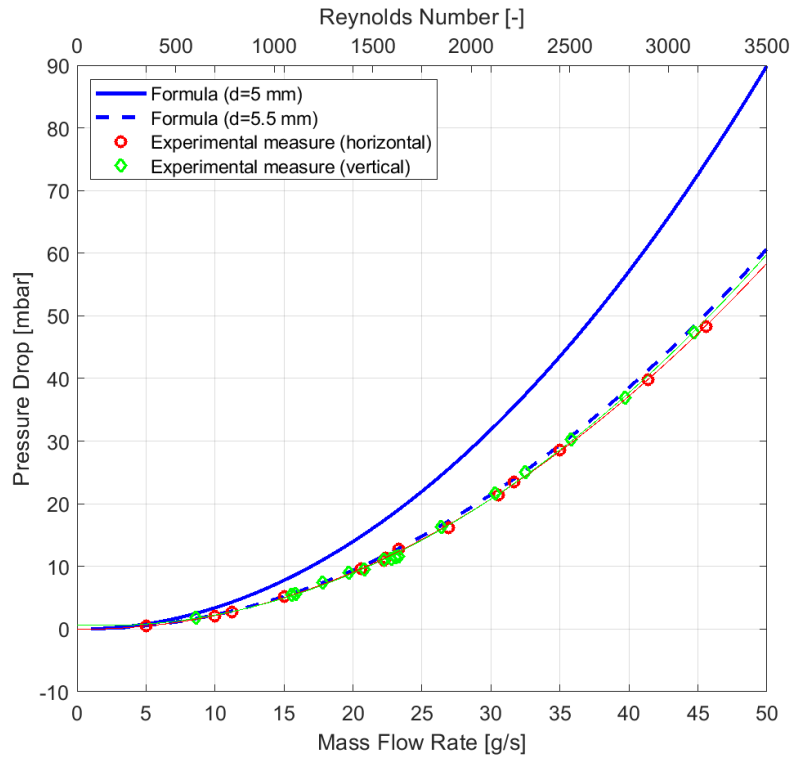
Figure 3. Orifice calibration curve

2.4. Test preparation and post-test procedure

The facility is filled with demineralized non-degassed water by opening valves V01 and V04 (Figure 1) and switching on the feeding pump until the water exits from valve V04. During this phase of forced circulation, all pressure transducers are purged in order to eliminate any eventual air from the transducers' chambers and the AISI 304 connection pipes (4 mm inner diameter, 6 mm outer diameter). Afterwards, valve V01 is closed and the pump is switched off.

This procedure also allows to eliminate air from the loop and the part of the UV below the horizontal pipe connecting to valve V04. On the other hand, the part of the vertical pipe connecting to safety valve V05 above valve V04 is still filled with air. This condition corresponds to the maximum possible filling of the facility, i.e. to 96.2% of the facility volume.

Tests with a lower mass of water and higher amount of air are carried out by discharging a defined amount of water through valve V03, while maintaining open valve V04 so that the pressure in the loop remains at the atmospheric value. The discharged mass is measured by a balance.

The mass of air present in the facility at the beginning of each experimental test depends on the volume initially occupied by the water and ambient temperature and pressure, which also influence the amount of air dissolved into the water.

Once the desired amount of water inside the facility is reached, valves V03 and V04 are closed.

Current to the electric heaters is regulated at the desired value to reach the chosen power, the DAS is started, 60 s later the electric heaters are turned on and the experimental test is carried out.

The test terminates when the power is switched off.

The facility then cools down and the following day, the water remaining in the facility is discharged through valve V02 and its mass is measured. This mass represents the mass inventory during the experimental test.

A series of water filling and water discharging tests at ambient temperature showed that the uncertainty on the water inventory can reach 10 g.

2.5. Test matrix, boundary and initial conditions

The boundary conditions of the tests are ambient temperature and pressure, and the power provided to the electric heaters, which starts at t=60 s. Initial conditions are defined by the walls and fluid temperatures, the water inventory in the loop and the liquid level in the HSWP.

The experimental tests setup consists in choosing the values of the power provided to the electric heaters, the water mass inventory in the loop and the initial liquid level in the HSWP, which has been fixed at 45 cm in the experimental tests here described.

The tests have been carried out by choosing the power provided to the electric heaters in a range from a 1300 W to a maximum of 5000 W approximately.

With reference to the water mass inventory, a loop Filling Ratio (FR) has been defined as the ratio between the volume of water initially present in the loop and the total volume of the facility ($3.123 \cdot 10^{-3}\,m^3$).

The mass of air present in the facility depends on the FR, and the initial ambient pressure and temperature. The explored range of FR is 0.507-0.962.

Some typical test parameters are reported in Table III. A liquid level is present in the facility at the beginning of the tests. When the closed loop is completely filled with water (FR=0.944), i.e. the liquid level is greater than 4.83 m, the amount of air present in the loop is the one dissolved into the water and only depends on the initial temperature and pressure (approximately 0.6 g at atmospheric pressure and 20°C). The initial value of the liquid level, measured from the bottom of the bayonet, are also reported in Table III. The liquid level is calculated considering the geometry of the facility and the water inventory and is confirmed by the values of the differential pressure Δp_2, Δp_3 and Δp_6 during the first 60 s of data acquisition.

All tests start from ambient temperature and pressure conditions, which are acquired during the first 60 s of each test.

At 60 s electric power is applied by a step increase of the electric voltage and heat is provided to the bayonet. No power regulation is carried out during each test. The duration of the tests depends on the pressure transient and temperature: in fact the power is switched off just before the pressure reaches a maximum value of 20 bar or when a steady-state condition is reached.

Table III. Experimental matrix

Electric Power [W]	FR	Loop water inventory [kg]	Air mass [10^{-3} kg]	Liquid level height [m]	Test time [s]	Initial temperature [°C]
1300	0.962	2.993	0.2268	4.946	18000	27.8
1700	0.962	2.998	0.2302	4.977	8180	25.6
2500	0.962	2.998	0.1957	4.975	3504	21.5
2500	0.911	2.838	0.4209	4.732	18000	21.6
2500	0.780	2.431	0.9051	4.126	18000	21.1
2500	0.645	2.007	1.3832	3.498	10800	26.0
2500	0.521	1.625	1.8695	2.925	18000	19.9
5000	0.911	2.841	0.4178	4.736	2833	21.3
5000	0.773	2.408	0.9306	4.092	18000	21.5
5000	0.643	2.006	1.4167	3.492	18000	19.7
5000	0.507	1.581	1.9112	2.860	18000	21.5

Depending on the boundary and initial conditions the experimental transients can have different possible evolutions:
- fast pressure increase and single-phase fluid in the loop, with short test duration due to the pressure that approaches 20 bar with a "diverging" behavior;
- single-phase flow in the loop, water boiling in the HSWP, pressures and temperatures that increase moderately; quasi-steady state conditions are reached in tests at low power;
- two-phase flow in the loop, boiling in the HSWP, pressure and temperatures that reach a quasi-steady state condition.

3. EXPERIMENTAL RESULTS

The typical experimental results are described in terms of time histories of fluid temperatures and pressures in the different regions of the loop.

The performance of the loop for the passive heat removal can be analyzed considering the rates of change of pressures and temperatures in the different points of the facility, which are affected by electric power and initial water inventory.

The pressurization rate, the heat-up rate and the capability of the system to reach steady-state conditions (dp/dt≈0; dT/dt≈0) depends on the loop characteristics (geometry, heat capacity, heat transfer surfaces, flow areas, etc.), initial and boundary conditions (mass inventory, initial temperature and power applied to the electric heaters), heat transfer effectiveness of the bayonet heat exchanger and of the heat sink, and the heat lost to the environment through the hot leg and cold leg.

The start-up phase of a natural circulation loop is influenced by the delays in the activation of specific heat transfer mechanism (convection, boiling, condensation) and mechanical non-equilibrium caused by local thermal perturbations.

The time evolution of pressure, wall and fluid temperatures, generically indicated hereafter with α, can be described by the product of two functions of the type f(α) and k(z,t):

$$\frac{d\alpha}{dt} = f(\alpha)k(z,t)$$

where z and t respectively represent the spatial coordinate along the loop and the time.

The spatial coordinate strongly influences the fluid temperature, while it has a smaller effect on the pressure. At the beginning of each test, depending on the FR, a liquid level is present either in the Upper Volume or in the loop. The regions above the liquid level are filled with air. The piece of pipe containing the orifice is completely full with water if the initial liquid level is greater than 1.62 m.

The values of electric power and FR define the phenomena occurring during the start-up transient and particular temporal phases. In tests at 1700/2500 W with FR>0.911, the heat-up of the bayonet and hot leg and the natural circulation start-up are accompanied by an exponential pressure increase, subcooled liquid flow along the whole loop, and natural convection with subcooled liquid in the HSWP. For FR<0.911, three temporal windows can be distinguished: the bayonet heat-up phase, the activation and development of natural circulation and the activation of the boiling in the HSWP.

The preliminary prediction of the phenomenological windows for each test, with the aim to classify them in advance, is not an easy task because of the particular geometry of the facility and the strong effects of applied electric power, initial liquid inventory and mass of air in the loop.

In most transients a nearly steady-state condition was reached; the transient is considered nearly steady-state when $d\bar{T}/dt$ is lower than 0.05°C/min over the last 10 minutes of the experiment. The average temperature $\bar{T}$ has been evaluated by a simple moving average, i.e. by taking the mean of the measured temperature over a period of time of 60 s.

The nearly steady-state condition is reached only when, from a certain time on, the power provided in the bayonet is transferred to the heat sink water pool and the environment. In this case, the pressure history shows an upward concavity at the beginning of the transient, then a flex occurs and the concavity changes (downward concavity).

In some tests, the water in the loop and in the pool remains subcooled along all the transient, the temperature difference between the fluid in the loop and in the pool is relatively small and natural convection occurs in the pool. Therefore, the power transferred to the pool is not sufficient to remove the power provided in the heat source. Consequently, the total internal energy in the system continues to increase and the pressure history shows an upward concavity.

When FR is greater than 0.944, the closed loop is completely filled with water: the liquid level is greater than 4.83 m and located in the UV already at the beginning of the test. The thermal expansion of the water due to the increase of its temperature, causes an increase of the volume occupied by the liquid and therefore an increase of the liquid level; the volume occupied by the air in the UV is reduced, and the pressurization rate increases during the time (upward concavity). This is the case for the tests at 1700 and 2500 W and FR=0.962.

In tests with similar filling ratio, the pressurization rate increases for higher applied electric power.

If the liquid level is initially lower than 4.83 m, air is initially present in the upper part of the loop; also in these tests the thermal expansion of the water causes an increase of the volume occupied by the water and therefore of the liquid level. Depending on the filling ratio, liquid and air may exit from the closed loop and enter the UV.

For small FRs (for example FR < 0.65), the volume occupied by the liquid remains lower than the closed loop volume during the tests. When the natural circulation starts, the air still present in the loop flows with the water and a two-phase two-component flow of water and air occurs.

With the increase of the temperature of the water, part of the air initially dissolved will separate from the liquid.

If the saturation temperature is reached in the loop, a multiphase (two-phase and two-component) flow of liquid water, steam and air occurs.

We assumed that water reaches saturation and two-phase flow occurs when the discrepancy between the fluid temperature and the saturation temperature is lower than 2°C. The chosen value represents the uncertainty on the temperature difference and takes into account the uncertainty of the measured temperature (approximately 1 K) and of the saturation temperature evaluated on the basis of the measured pressures (uncertainty of approximately 0.3 bar).

After 60 s of initial steady-state phase at zero electric power, each transient can be divided in the following phenomenological windows: heat-up of the bayonet, natural circulation activation, natural circulation development and nearly steady-state natural circulation.

During the initial condition phase, zero power is provided to the bayonet and the acquired signals are used to evaluate the initial standard deviation for each parameter.

The heat-up phase of the bayonet starts at 60 s when electric heaters are switched on. During this phase a rapid increase of temperature of the bayonet wall and of the fluid at the bayonet outlet (T2) is observed. The end of this phase is conventionally fixed at the time when the rate of increase of bayonet outlet temperature (T2) strongly reduces; in single-phase tests the rate becomes negative for some time, therefore a relative maximum is present.

The next phase is the one of natural circulation activation. The end of the phase is conventionally fixed at the time when hot fluid exiting the bayonet manages to travel along the loop and reaches the bayonet inlet, i.e. when the temperature T8 starts to increase; the temperatures in the hot leg (T3,4,5) and at the heat sink tube outlet (T6) increase during the natural circulation activation phase.

During both the heat up and the natural circulation activation phases, U-tube instabilities can occur in the loop; they are witnessed by oscillating pressure drop and flow reversal through the orifice; the temperature at the bayonet inlet T8 (and sometimes even at the orifice inlet T7) increases with an oscillating behaviour.

In this phase the heat sink is not active, since the same fluid temperature is present in the pool and in the heat sink pipe.

The oscillations occurring during the tests depend on the electric power, the subcooling at the bayonet inlet and the ratio between the air mass present in the upper plenum and the total mass of air present in the facility. For low FR, a considerable amount of air that flows in the loop, a two-phase two-component mixture of air and water is present in the loop, and the flow patterns can strongly influence both pressure drops and flow rate, especially at low pressure.

During the phase of development of the natural circulation, water temperatures in the hot and cold legs still increase with a different rate; consequently also natural circulation driving force and flow rate increase. This phase ends when the flow rate reaches a nearly steady-state value.

The following phase is the nearly steady-state natural circulation; this phase is not reached in test at high FR, precisely at FR=0.962 with any power greater than 1300W, and at FR=0.911 with power 5000 W.

During the phases of development and nearly steady-state natural circulation, two-phase instabilities occur especially at low FR: wide oscillations of the pressure drop across the orifice (and therefore, flow rate) are present, together with significant oscillations of the temperatures in the cold leg, absolute and differential pressures.

Some typical time behaviours of temperatures and pressures are here analysed, namely the ones of the tests at 2500 W and FR of 0.962 and 0.645, and for a test at 5000 W and FR=0.643.

3.1. Test at 2500 W and Filling Ratio equal to 0.962

The experimental results are shown in Fig. 4a-f. Single-phase circulation occurs in this test and the pressure reaches values very close to the safety valve opening pressure while the water is still highly subcooled. The pressurization rate increases with time and the pressure time history (Fig. 4a) shows an upward concavity ("diverging" behaviour) as an effect of the thermal expansion of the liquid water. The test is stopped before the opening of the safety valve.

The temperatures time behaviors (Fig. 4b-c) are typical of tests with single-phase natural circulation.

During the bayonet heat-up phase (60-270 s), the temperature at the bayonet outlet (T2) increases up to a maximum. The temperature T3 at the riser inlet starts to increase and reaches a maximum with some delay (50-70 s). Up to approximately 120 s, the flow rate across the orifice (Fig. 4d-e) shows oscillations around zero, showing that flow of fluid occurs in both directions, but without any net mass transfer.

These oscillations cause the entrance and mixing of some hot water from the annulus in the inversion chamber and, together with conduction, convective motions induce a small increase of the temperature in the bayonet inversion chamber (T1), followed by a decrease when a net downward motion of fluid in the downcomer occurs and colder water enters the chamber. In this phase the water pool is not active as heat sink, since the temperature of water inside the tube is still equal to the one of the water in the pool.

During the natural circulation activation phase (270-340s), an initial reduction of T2 and T3 is observed when cold fluid enters the bayonet inversion chamber and annulus, and moves upward along the hot leg.

The natural circulation development phase starts at 340 s, when the temperature at the bayonet inlet increases, and lasts up to the end of the experiment. After approximately 500 s, all the temperatures are increasing with a rate that diminishes with time; nevertheless, a nearly steady-state condition is not reached. As far as the water pool is concerned, it seems inactive up to 440 s. Afterwards the water temperature increases (Fig. 4f), but the water is highly subcooled and heat is transferred to the pool with a small efficiency due to natural convection. The presence of thermal stratification is evident, since the temperature in its bottom part (TP3) is 20-25°C lower than in the upper part (TP1).
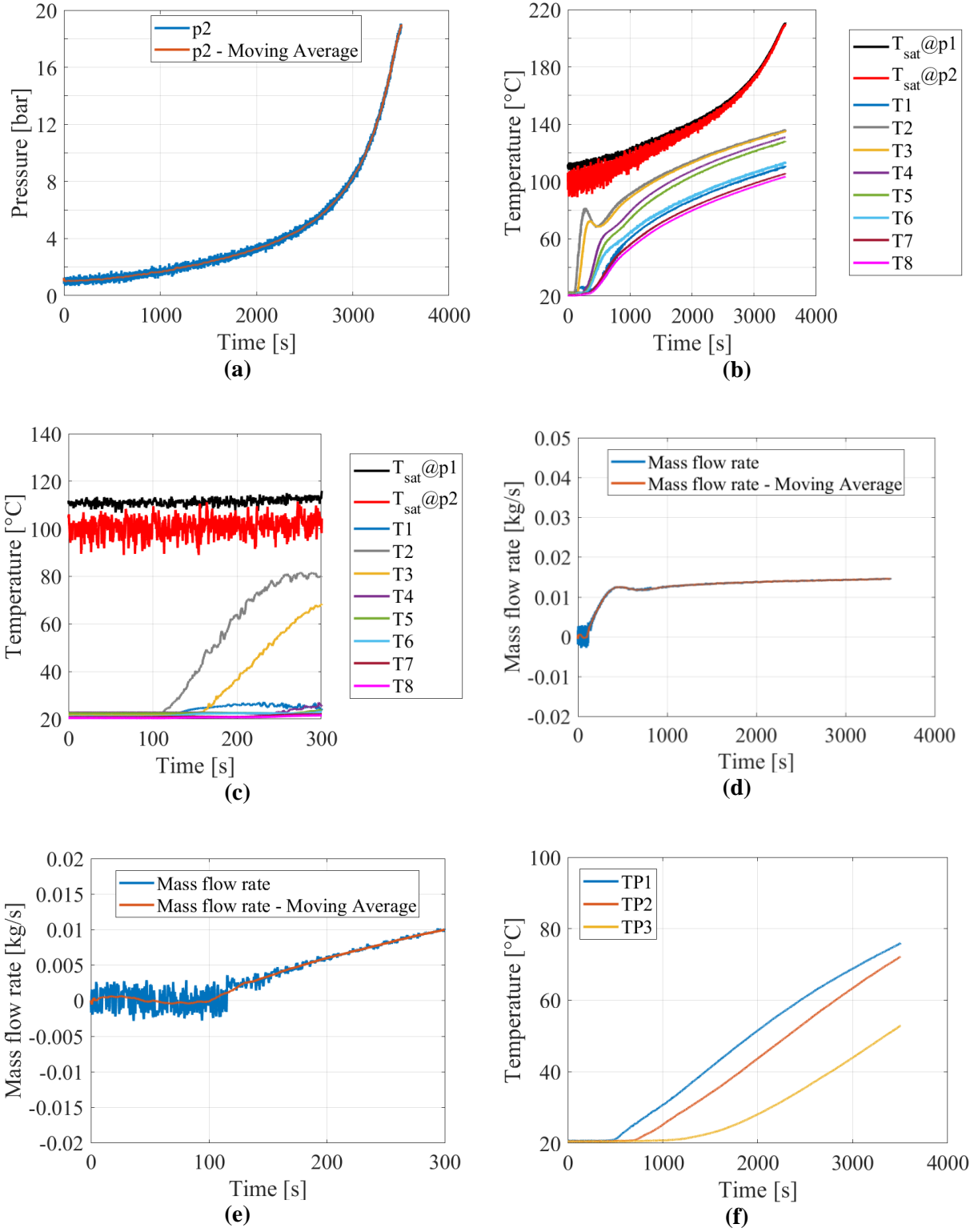
Figure 4. Test at 2500 W and FR=0.962: a) absolute pressure; b), c) fluid temperatures in the loop; d), e) estimated flow rate in the loop; f) pool water temperature.

3.2. Test at 2500 W and Filling Ratio equal to 0.645

The time histories of pressures and temperatures are shown in Fig. 5a-h. Both pressure and temperature in the loop reach nearly steady-state conditions after approximately 5000 s.

The heat-up phase lasts from 60 s to 450 s. In this phase temperatures T2 and T3 at the bayonet outlet reach the saturation value and T1 approaches it.

Wide and frequent (~0.5 Hz) flow rate oscillations between positive and negative values are observed between 230 s and 450 s. The amount of water that moves from the bayonet annulus to the downcomer (reverse flow) is enough to reach the bayonet inlet; therefore, temperatures T8 and T7 increase (with some oscillations), even though the water in the cold leg (T5 and T6) is still at the initial temperature. During the natural circulation activation phase, which ends at approximately 810 s, flow rate oscillations are characterized by different amplitude and shape. Figure 5g shows the flow rate behaviour between 600s and 800 s: smaller oscillations are superimposed to wider oscillation.

The sharp peaks of the temperature T8 at the bayonet inlet occur just in correspondence of the negative peaks of flow rate. The temperatures T2 and T3 reach the saturation value at 270 s and 380 s respectively. The natural circulation development phase ranges from 810 s to 5800 s. During this phase the saturation temperature is reached at the top of the riser (T4) at 1500 s and at the heat sink tube inlet (T5) at 4000 s.

Wide amplitude flow rate oscillations are present in this phase, but the time-averaged values increase and are positive, so that a net mass transfer from the bayonet to the heat sink occurs.

After 4000 s, condensation occurs inside the heat sink pipe, while previously subcooled forced convection occurred. With this small FR, two-phase two-component (water and air) flow occurs in the loop and oscillations are present in pressures and temperatures.

Temperature in the bayonet inversion chamber (T1) shows patterns of oscillations with a time period of approximately 15 s. Temperature in the water pool increases: saturation is reached at 5000 s in the upper region and at 5800 s in the lower region. At this time saturated pool boiling occurs on the whole outer surface of the heat sink pipe.

During the nearly steady-state phase, the high heat transfer coefficient in the pool and the high values of fluid temperature difference between the inner and outer side of the heat sink pipe allow to avoid further increase of pressure and temperatures.

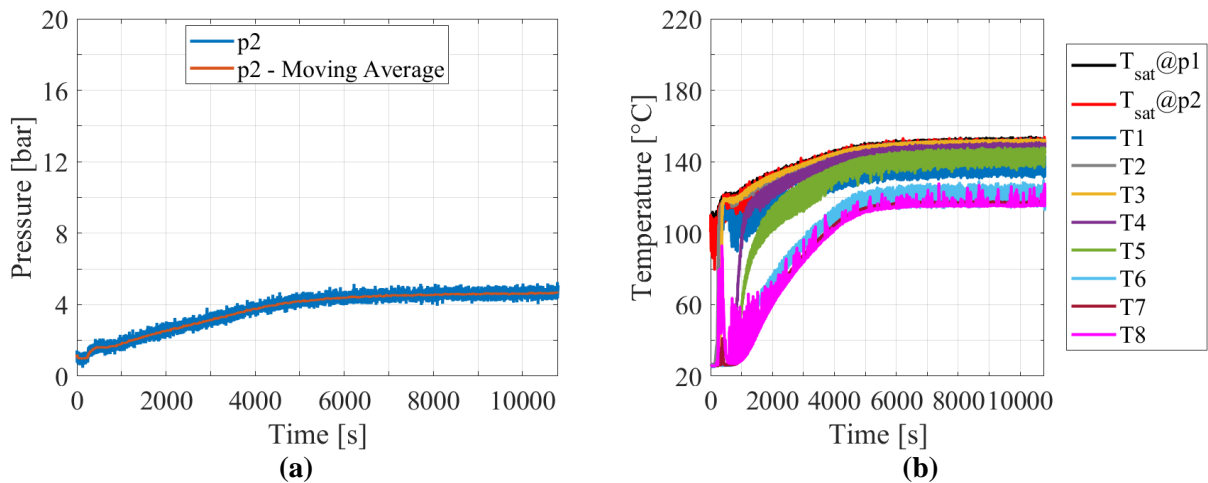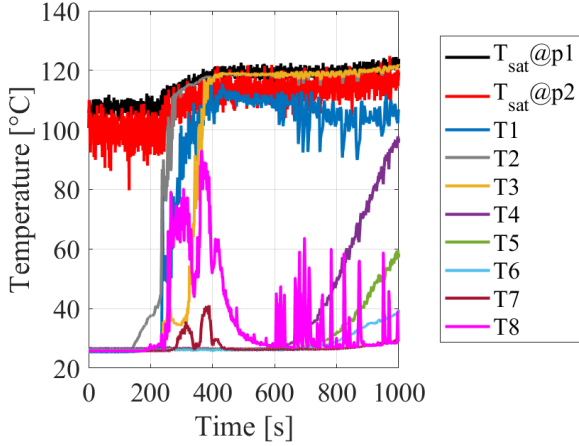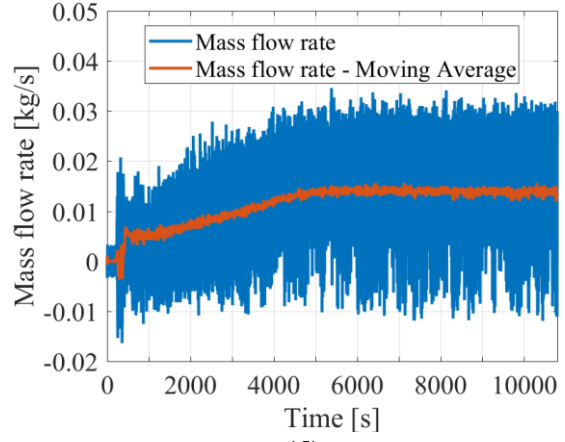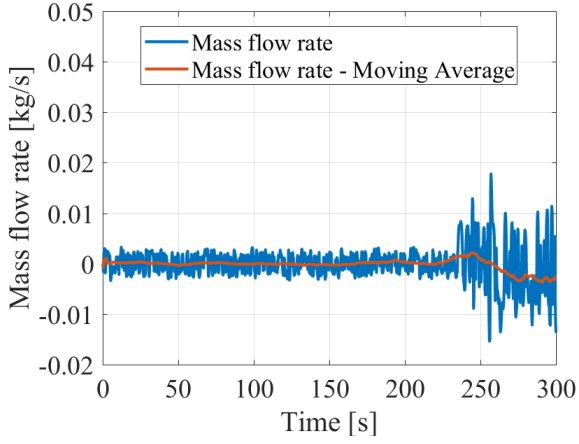**(a)**   **(b)**

Figure 5. Test at 2500 W and FR=0.645: a) absolute pressure; b), c) fluid temperatures in the loop; d), e), f), g) estimated flow rate in the loop; h) pool water temperature.

Figure 5 (continued). Test at 2500 W and FR=0.645: a) absolute pressure; b), c) fluid temperatures in the loop; d), e), f), g) estimated flow rate in the loop; h) pool water temperature.
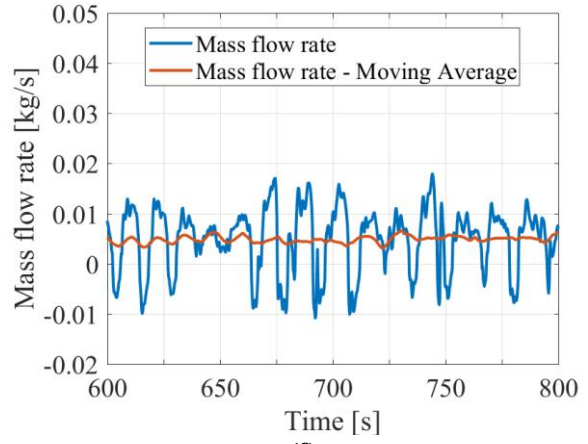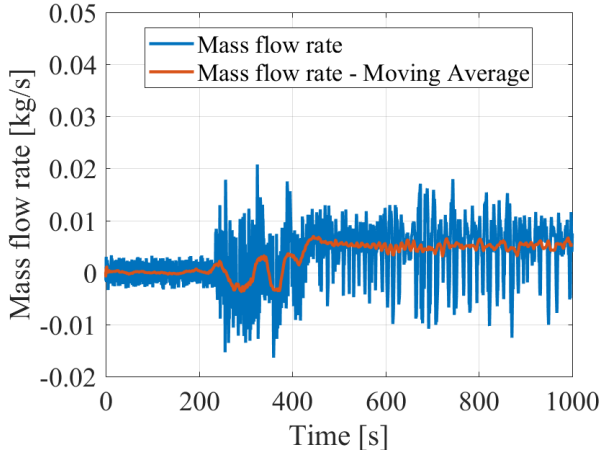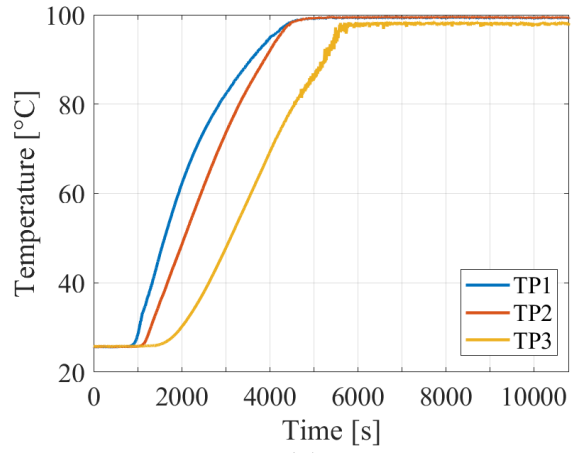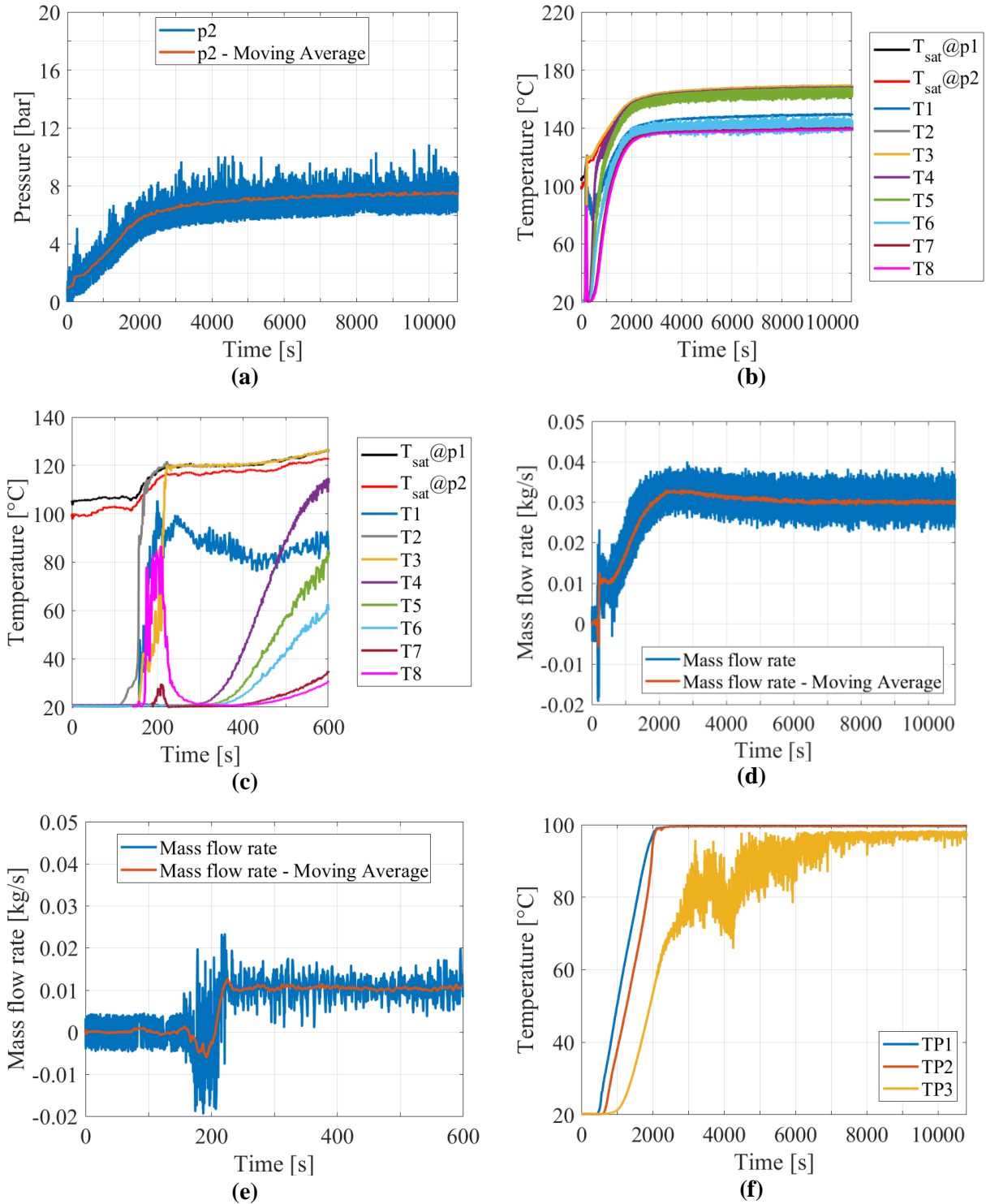
16

Figure 6. **Test at 5000 W and FR=0.643: a) absolute pressures; b), c) fluid temperatures in the loop; d), e) estimated flow rate in the loop; f) fluid temperatures in the pool.**

In general, pressure oscillations are observed, which are typical of the occurrence of two-components (air and water) two-phase flow at relatively low pressure. Temperature oscillations are probably linked to the presence of non-equilibrium phenomena between the liquid phase (water) and gaseous phase (mixture of steam and air).

3.3. Test at 5000 W and Filling Ratio equal to 0.643

Figures 6a-f represent the time histories of temperatures, pressures and flow rate.
The heat-up phase is somewhat shorter than in the previous test and ends at 220 s. The time histories of the fluid temperatures in the loop are of the same type as in the previous test; on the other hand, until 165 s the flow rate oscillates around zero with a long period. At 190 s a quite wide negative peak of flow rate occurs, and it is accompanied, similarly to the previous test, by the increase of the temperature T8 at the bayonet inlet beyond 80°C and a small increase of T7, while the water in the cold leg (T6) is still at 20°C.
Much lower flow rate instabilities occur in this test. The end of natural circulation activation phase is identified at approximately 400 s. The temperatures T7 and T8 at the bayonet inlet decrease and reach again the initial value, then they start to increase at 400 s. The temperatures T2 and T3 reach the saturation value at 170 s and 205 s respectively.
The natural circulation development phase is assumed to finish at 3500 s, when a reduction of the pressurization rate occurs. In fact, even though after 3500 s pressure and temperatures continuously increase, their rate of change is so small that they can be considered nearly steady-state.
During this phase, the saturation temperature is reached in all the hot leg: T2, T3, T4 and T5 reach saturation respectively at 170 s, 205 s, 1000 s and 1800 s. The flow rate increases and reaches a relative maximum at 2500 s.
At 2100 s, most of the HSWP is at saturation temperature; heavy boiling occurs and the evaporated water is reintegrated by cold water provided by the water reservoir (WR). The entrance of this water causes temperature fluctuations in the lower region of the HSWP, which is still subcooled in this phase.
During the nearly steady-state natural circulation phase, the power transferred to the HSWP and to the environment is somewhat smaller than the power received in the bayonet and therefore pressure and temperature are slightly increasing.
On the other hand, the flow rate reaches an almost constant value. The time-averaged final value seems greater than in the test at 2500 W (0.03 kg/s against 0.016 kg/s). It must be noted that flow rates have been derived from the pressure drop across the orifice assuming single-phase liquid. In tests with low FR, air is dragged along the loop and also through the orifice. If this occurs, two-phase flow should be considered and the actual value of water flow rate would be lower than the value calculated for single-phase liquid. Therefore, the flow rate reported in Fig. 5d and 6d should be considered only qualitatively and not quantitatively.

3.4. Effect of power and Filling Ratio on the experimental results

Table IV reports the end time of the heat-up phase, natural circulation activation phase, natural circulation development phase, the time when saturation condition is reached in the upper part of the HSWP, the final pressure and the final state reached in each test.
The end of the natural circulation development, which corresponds to the time when the average flow rate becomes constant, occurs at similar times (approximately 6000 s) for all the test at 2500 W.
Increasing the power, the natural circulation is established more quickly and lower flow instabilities are observed. In the test with 5000 W and FR lower than 0.911, nearly-steady state conditions are reach after 3000-4000 s.
Table IV also shows that the final pressure increases with increasing power and increasing FR values.
The values of pressure and temperatures reached in the tests at fixed times are reported in Table V.

It is important to highlight that the tests with diverging pressure are characterized by the development of single-phase natural circulation. In the other tests with lower FR, two-phase natural circulation occurs: saturation temperature is reached in the hot leg and the amount of air mixed with the coolant is no longer negligible. In these cases, both air and steam contribute to the pressure in the loop.

The fluid temperature at the bayonet outlet (T2) decreases for decreasing FR values and increases for increasing power.

The flow rate at the end of the experimental transients with power 2500 W is in the range 0.014-0.016 kg/s and is weakly influenced by the FR value. On the other hand, the power visibly affects the final flow rate: the flow rates in the tests at 5000 W reaches values that are approximately the double of the ones in the tests at 2500 W. Nevertheless, in tests were air is present in the loop, a two-phase flow occurs through the orifice and the correlations used for the flow rate evaluation (reported in section 2.3 and valid only in single-phase flow) may cause an overestimation. Therefore, in these tests, only the qualitative behavior of the flow rate can be considered.

Finally, figures 7a, 7b and 7c show some typical temperature profiles along the curvilinear coordinate of the loop at different times of the transient. The curves approach each other when quasi-steady state conditions are reached, as shown in figures 7b and 7c for the tests with low FR.

Figure 7a shows that nearly-steady state conditions are not reached: this fact occurs in all the tests at high filling ratio characterized by the presence of single-phase liquid in the loop.

The slope of the curves is proportional to the power received/lost by the fluid. Especially during the heat-up, natural circulation activation, but partially also during the natural circulation development phases, the solid structures are not in thermal equilibrium with the fluid. Therefore, the slope of the temperature axial profile depends also on the heat that is absorbed and stored in the solid structures.

At the end of the experimental tests characterized by nearly-steady state conditions, slopes are linked only to the electric power provided to the bayonet, the heat lost to the environment along the pipes and the power delivered to the HSWP.

The pictures clearly show that, at the end of the transient, the fluid flowing downward in the downcomer (region marked in Fig. 7 with the term "BHX downc.") is "pre-heated" by the fluid flowing up in the annular region of the bayonet ("BHX ann." in Fig. 7), i.e. a sort of "regenerative" heat exchange occurs.

Table IV. End time of the different phases

Power [W]	FR	Heat-up end [s]	Natural circulation activation end [s]	Natural circulation develop-ment end [s]	HSWP saturation time [s]	Final state	Final pressure [bar]
1300	0.962	330	400	-	-	Not steady-state	9.97
1700	0.962	320	345	-	-	Diverging pressure	
2500	0.962	270	340	-	-	Diverging pressure	
	0.911	330	390	5800	5300	Not steady-state	7.47
	0.780	250	750	6000	4500	Not steady-state	5.14
	0.645	450	810	5800	4700	Steady-state	4.94
	0.521	570	1000	6000	4800	Steady-state	4.84
5000	0.911	210	280	-	2700	Diverging pressure	
	0.773	220	380	4000	2250	Not steady-state	13.85
	0.643	240	400	3000	2000	Steady-state	7.52
	0.507	280	450	3000	2100	Steady-state	7.22

Table V. Values of pressure and temperatures at fixed times

| Power [W]	FR	Time [s]	P2 [bar]	T1 [°C]	T2 [°C]	T5 [°C]	T6 [°C]	T8 [°C]	W [g/s]
1300	0.962	1800	1.7	60	82	73	64	57	10.4
		3600	2.4	79	98	92	82	75	10.9
		7200	4.2	100	117	113	103	96	11.3
		10800	6.5	110	126	122	113	105	11.4
1700	0.962	1800	2.1	66	89	78	67	60	11.3
		3600	3.5	88	109	102	90	82	12.1
		7200	15.9	112	130	126	116	106	12.8
2500	0.962	1800	2.9	83	110	99	86	76	13.5
		3500	18.9	110	135	128	113	103	14.5
	0.911	1800	1.9	87	116	105	91	81	14.2
		3600	3.5	123	141	135	123	114	17.3
		7200	6.2	139	160	157	139	131	16.0
		10800	6.5	138	161	158	139	131	15.8
	0.780	1800	2.4	110	129	97	72	54	9.2
		3600	3.6	125	142	128	109	96	11.5
		7200	4.7	135	151	142	124	116	14.5
		10800	4.9	136	153	144	125	116	14.4
	0.645	1800	2.4	110	130	105	68	55	6.5
		3600	3.5	124	143	130	104	96	11.0
		7200	4.5	135	150	142	120	116	14.0
		10800	4.65	136	151	143	120	116	14.0
	0.521	1800	2.6	110	130	107	70	62	10.0
		3600	3.8	125	143	134	105	100	15.0
		7200	4.7	135	152	144	119	115	16.0
		10800	4.75	136	152	145	119	116	16.0
5000	0.911	1800	9.0	148	174	163	146	134	21.7
		2800	18.5	161	195	188	161	150	20.5
	0.773	1800	6.0	147	161	158	152	144	43.7
		3600	12.5	175	191	190	175	168	36.5
		7200	13.3	175	194	193	175	167	32.5
		10800	13.7	175	195	194	176	168	32.0
	0.643	1800	5.3	136	156	149	131	126	29.5
		3600	6.75	146	165	161	139	136.5	31.5
		7200	7.3	149	168	165	141	138	30.0
		10800	7.5	149	169	165	142	139	30.0
	0.507	1800	5.5	140	158	154	134	130	29.0
		3600	7.0	150	166	164	143	141	32.7
		7200	7.3	152	169	166	144	142	31.0
		10800	7.4	153	169	167	145	143	31.0
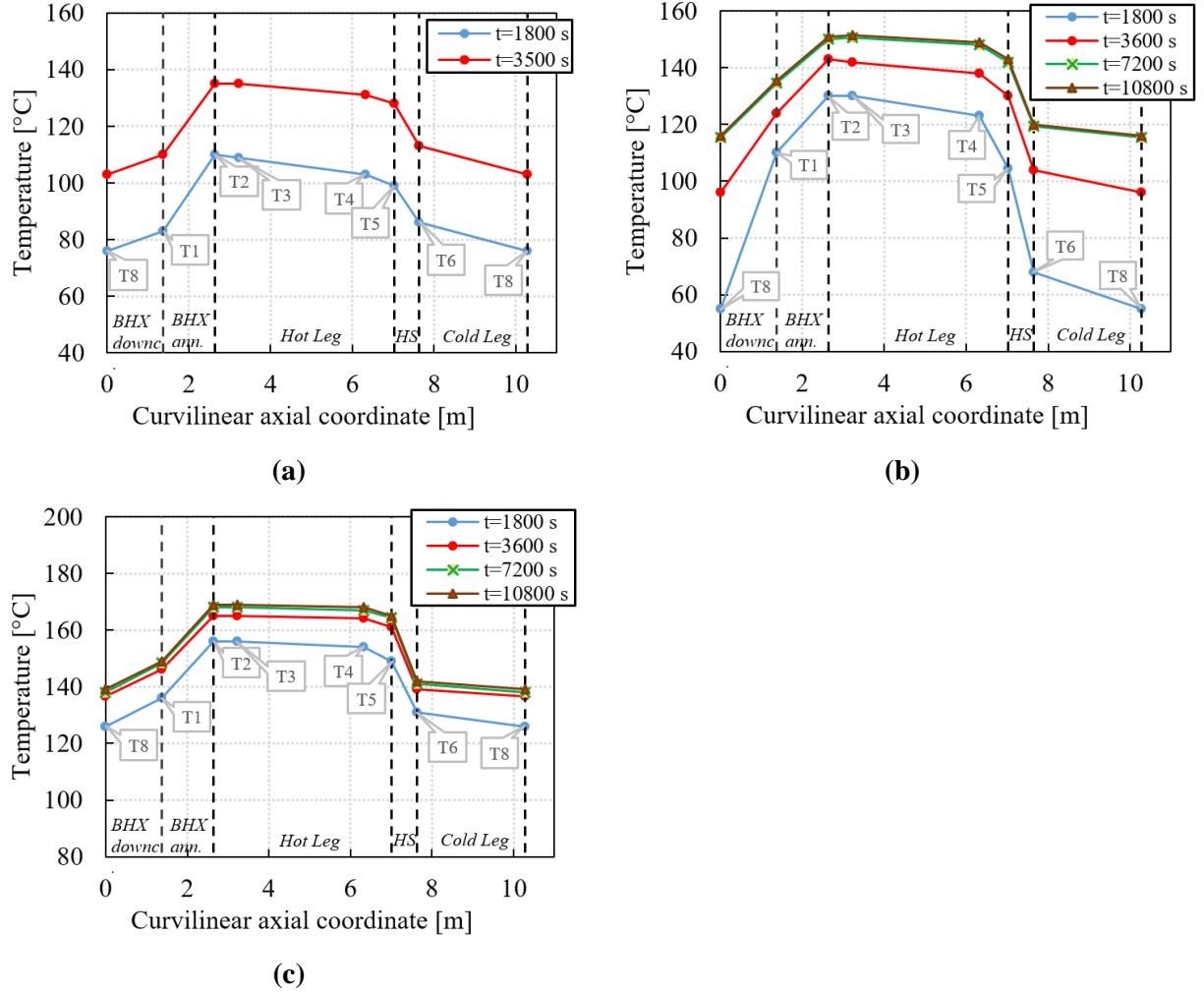
Figure 7. Curvilinear temperature profile along the loop: a) 2500 W, FR=0.962; b) 2500 W, FR=0.645, c) 5000 W, FR=0.643

4. CONCLUSIONS

The experimental campaign concerns the start-up of a natural circulation loop in single and two-phase flow. The effect of the heat source power and initial mass inventory have been investigated. The time histories of pressures, temperatures and flow rate allowed to define characteristics phases during the start-up transient. The bayonet heat-up phase duration increases for decreasing values of FR and of the electric power. Times of natural circulation activation and development have been analyzed in all tests. A nearly steady-state condition is reached only in the tests with lower FR values.

Increasing the power, the natural circulation is established more quickly; the final pressure increases with the power and decreases with the FR value. The natural circulation flow rate at the end of the experimental transients has been estimated and it is consistently dependent on the heat source power, with a small influence of the FR value.

An accurate thermal analysis of the experimental results is ongoing and the effect of loop geometry and heat sink will be studied also numerically by system codes such as Relap5. The use of Relap5 will also allow to evaluate void fractions and qualities along the loop and the fraction of air versus steam in the gaseous phase when two-phase flow occurs.

21

REFERENCES

1. T.L. Schultz, 2006. Westinghouse AP1000 advanced passive plant. Nucl. Eng. Des. 236, 1547-1557.
2. A.J. Barrett and W. Marquino, 2012. ESBWR response to an extended station blackout/loss of all AC power. Proceedings of the ICAPP'2012 International Congress on Advanced Nuclear Power Plants, Chicago, IL (USA), June 24-28, 2012, pp. 30-36.
3. W. Zhou et al, 2013. Assessment of RELAP5/MOD3.3 condensation models for the tube bundle condensation in the PCCS of ESBWR, Nucl. Eng. Des. 264, 111–118.
4. Z. Liu and J. Fan, 2014. Technology readiness assessment of Small Modular Reactors. Progr. Nucl. Energy 70, 20-28.
5. Generation IV Technical Forum, Technology Roadmap Update for Generation IV Nuclear Energy Systems, 2014
6. Yoram Zvirin, 1981. A review of natural circulation loops in pressurized water reactors and other systems. Nucl. Eng. Des. 67, 203-225.
7. P.K.Vijayan, H.Austregesilo, 1994. Scaling laws for single-phase natural circulation loops. Nucl. Eng. Des. 152, 331-347.
8. P.K.Vijayan, H.Austregesilo, 1995. V.Teschenorff, Simulation of the unstable oscillatory behavior of single-phase natural circulation with repetitive flow reversals in a rectangular loop using the computer code ATHLET. Nucl. Eng. Des. 155, 623-641.
9. P.K.Vijayan, 2002. Experimental observations on the general trends of steady state and stability behavior of single-phase natural circulation loops. Nucl. Eng. Des. 215, 139-152.
10. B.T. Swapnalee, P.K. Vijayan, 2011. A generalized flow equation for single phase natural circulation loops obeying multiple friction laws. Int. J. Heat Mass Transf. 54, 2618-2629.
11. Kumar Naveen, Kannan N. Iyer, J.B. Doshi, P.K. Vijayan, 2014. Investigations on single-phase natural circulation loop dynamics. Part2: role of constitutive laws. Prog. Nucl. Energy 75, 105-116.
12. S.M.Seyyedi, N. Sahebi, A.S. Dogonchi, M. Hashemi-Tilehnoee, 2019. Numerical and experimental analysis of a rectangular single-phase natural circulation loop with asymmetric heater position. Int. J. of Heat Mass Transf. 130, 1343-1357.
13. A. Pini, A. Cammi, L. Luzzi, 2016. Analytical and numerical investigation of the heat exchange effect on the dynamic behavior of natural circulation with internally heated fluids. Chem. Eng. Sc. 145, 108-125.
14. J.A. Boure et al, 1973. Review of two-phase flow instability. Nucl. Eng. Des. 25 (2), 165–192.
15. E. Manavela Chiapero, M. Fernandino, C.A. Dorao, 2012. Review of pressure drop oscillations in boiling systems. Nucl. Eng. Des. 250, 436-447.
16. L.C. Ruspini, C.P. Marcel, A. Clausse, 2014. Two-phase flow instabilities: a review. Int. J. Heat Mass Transf. 71, 521-548.
17. Kun Cheng, Tao Meng, Sichao Tan, Zheng Liu, 2019. Experimental study on natural circulation flow instability in parallel boiling channels under low pressure. Int. J. Heat Mass Transf. 132, 1126-1136.
18. G. Su et al, 2002. Theoretical and experimental study on density wave oscillation of two-phase natural circulation of low equilibrium quality, Nucl. Eng. Des. 215, 187–198.
19. Zhiee Jhia Ooi, Vineet Kumar, Caleb S. Brooks, 2019. Experimental database of two-phase natural circulation with local measurements. Progr. Nucl. Energy 116, 124-136.
20. Qiang Wang et al., 2019. Numerical simulation of thermal-hydraulic characteristics in a closed natural circulation system. IOP Conf. Series: Earth and Environmental Science 227 022001.

21. O N Kabankov, L A Sukomel, V V Yagov, N O Zubov, 2019. Experimental study of hydrodynamics and heat transfer in two-phase natural circulation loop with reference passive cooling systems of nuclear power plants. J. of Physics: Conference Series 1370, 012055.
22. A. Manera and T.H.J.J. van Der Hagen, 2003. Stability of natural-circulation-cooled boiling water reactors during startup: experimental results. Nucl. Technol. 143, 77–88.
23. M. Furuya et al., 2005. Flashing-induced density wave oscillations in a natural circulation BWR-mechanism of instability and stability map. Nucl. Eng. Des. 235, 1557–1569.
24. K. Woo, 2008. Experimental and Analytical Study of Stability Characteristics of Natural Circulation Boiling Water Reactors during Startup Transients. Dissertation, Purdue University.
25. A. Dixit et al., 2013. Startup Transient Test Simulation with and without void reactivity feedback for a two-phase natural circulation reactor. Nucl. Eng. Des. 265, 1131-1147.
26. S. Shi et al, 2015. Experimental investigation of natural circulation instability in a BWR-type small modular reactor. Prog. Nucl. Energy 85, 96–107.
27. S. Shi et al., 2016. Startup instability in natural circulation driven nuclear reactors, Prog. Nucl. Energy 90, 140-150.
28. S.Y. Jiang et al, 1995.Experimental simulation study on startup of the 5 MW nuclear heating reactor. Nucl. Eng. Des., 158, 111–123.
29. Xing Lv et al., 2016. Design Analysis of a new passive residual heat removal System. Nucl. Eng. Des. 303, 192-202.
30. Yeon-Sik Kim, et al., 2016. Application of direct passive residual heat removal system to the SMART reactor. Annals Nucl. Energy 89, 56-62.
31. D.C. Sun, et al., 2018. Experimental investigation on natural circulation characteristics of emergency passive residual heat removal system in WPR1000. Progr. Nucl. Energy 103, 1-7.
32. S. Shi et al., 2018. Assessment of Relap5/Mod3.2 for startup transients in a natural circulation test facility. Annals Nucl. Energy 112, 257-266.
33. A.Fakhraei, F.Faghihi, A. Rabie, M.Safarina, 2021. Coolant flow rate instability during extended station blackout accident in NuScale SMR: Two approaches for improving stability. Progr. Nucl. Energy 131, 103602.
34. C. Bertani et al., 2017. Preliminary numerical studies of an experimental facility for heat removal in natural circulation. J. of Physics: Conference Series 796, 012046.
35. C. Bertani et al., 2020. Experimental study of natural circulation loop and RELAP5-3D analysis. *J. Phys.: Conf. Ser.* 1599, 012021.
36. C. Bertani et al., 2017. Verification of RELAP5-3D code in natural circulation loop as function of the initial water inventory. J. of Physics: Conference Series 923, 012008.
37. M. Caramello et al., 2017. Thermal-hydraulic analysis of passively controlled DHR System. Prog. Nucl. Energy 99, 127-139.
38. V. Narcisi et al., 2020. Preliminary evaluation of ALFRED revised concept under station blackout. Nucl. Eng. Des. 364, 110648.
39. P.K. Vijayan et al., 1994. Scaling laws for single-phase natural circulation loops. Nucl. Eng. Des 152, 331-347.
40. M. Ishii and I. Kataoka, 1984. Scaling laws for thermal-hydraulic system under single phase and two-phase natural circulation. Nucl. Eng. Design 81, 411-425.
41. A. Brunelli, 2015. Manuale di strumentazione: misura e controllo dei sistemi industriali. Hoepli.it, 116.